


## ORIGINAL RESEARCH

# Improved fire severity mapping in the North American boreal forest using a hybrid composite method

Lisa M. Holsinger<sup>1</sup> , Sean A. Parks<sup>1</sup>, Lisa B. Saperstein<sup>2</sup>, Rachel A. Loehman<sup>3</sup>, Ellen Whitman<sup>4</sup>, Jennifer Barnes<sup>5</sup> & Marc-André Parisien<sup>4</sup>

<sup>1</sup>Aldo Leopold Wilderness Research Institute, Rocky Mountain Research Station, US Forest Service, 790 E. Beckwith Ave., Missoula Montana, 59801,

<sup>2</sup>US Fish and Wildlife Service, 1011 E. Tudor Rd., Anchorage Alaska, 99503,

<sup>3</sup>US Geological Survey, Alaska Science Center, University Drive, Anchorage Alaska, 99503,

<sup>4</sup>Natural Resources Canada, Canadian Forest Service, Northern Forestry Centre, 6520-122 Street, Edmonton Alberta, T6H 3S5, Canada

<sup>5</sup>National Park Service, Alaska Regional Office, 4175 Geist Rd., Fairbanks Alaska, 99709,

## Keywords

Boreal forests, burn severity, Composite Burn Index, dNBR, RBR, fire severity, Google Earth Engine

## Correspondence

Lisa M. Holsinger, Aldo Leopold Wilderness Research Institute, Rocky Mountain Research Station, US Forest Service, 790 E. Beckwith Ave., Missoula, MT 59801.

Tel: 406-542-4172; Fax: 406-542-4196;

E-mail: lisa.holsinger@usda.gov

Editor: Mat Disney

Associate Editor: Stephanie Bohlman

Received: 19 May 2021; Revised: 23 August 2021; Accepted: 31 August 2021

doi: 10.1002/rse2.238

*Remote Sensing in Ecology and Conservation* 2022; **8** (2):222–235

## Abstract

Fire severity is a key driver shaping the ecological structure and function of North American boreal ecosystems, a biome dominated by large, high-intensity wildfires. Satellite-derived burn severity maps have been an important tool in these remote landscapes for both fire and resource management. The conventional methodology to produce satellite-inferred fire severity maps generally involves comparing imagery from 1 year before and 1 year after a fire, yet environmental conditions unique to the boreal have limited the accuracy of resulting products. We introduce an alternative method – the ‘hybrid composite’ – based on deriving mean severity over time on a per-pixel basis within the cloud-computing environment of Google Earth Engine. It constructs the post-fire image from satellite data composited from all valid images (i.e., clear-sky and snow-free) acquired in the time period immediately after fire through the early growing season of the following year. We compare this approach to paired-scene and composite approaches where the post-fire time period is from the growing season 1 year after fire. Validation statistics based on field-derived data for 52 fires across Alaska and Canada indicate that the hybrid composite method outperforms the other approaches. This approach presents an efficient and cost-effective means to monitor and explore trends and patterns across broad spatial domains, and could be applied to fires in other regions, especially those with frequent cloud cover or rapid vegetation recovery.

## Introduction

Wildfire is the dominant disturbance agent in North American boreal forests (Kasischke et al., 2010; Randerson et al., 2006), a biome of over 6 million km<sup>2</sup> containing the highest proportion of intact forest on Earth (Potapov et al., 2017; Venier et al., 2018; Watson et al., 2018; Wells et al., 2020). The ‘severity’ of wildfires, defined here as the degree of fire-induced ecological change to vegetation, dead biomass, and soil (Eidenshink et al., 2007; Kolden & Rogan, 2013), fundamentally shapes the structure and function of boreal ecosystems at a range of temporal and spatial scales. For example, fire severity influences landscape-level vegetation patterns, post-fire successional

trajectories, permafrost dynamics, soil erosion, carbon dynamics, wildlife habitat, and subsistence resources (Balshi et al., 2007; Johnstone et al., 2010; Minsley et al., 2016; Thom & Seidl, 2016; Whitman, Whitman, et al., 2019). Because fire severity plays such a pivotal role in boreal forests, spatially explicit data describing severity patterns are essential to our understanding of ecological processes in these fire prone ecosystems. Much of the North American boreal forest, however, lies in remote and inaccessible areas where wildfires are not easily monitored on the ground (Duffy et al., 2007; Hawbaker et al., 2017). Remote sensing offers repeat observations over multi-decadal time periods and provides a powerful tool for monitoring and studying fire across the vast boreal biome.

Multispectral imagery, such as Landsat data, has been widely used in research and management to characterize fire effects due to its ability to isolate signals directly resulting from fire (Chen et al., 2021). Spectral imagery from before and after a fire can be compared and integrated into indices (e.g. the differenced normalized burn ratio, dNBR) that detect surface changes, such as vegetation mortality, char, moisture loss, and soil erosion (White et al., 1996). Related, ground-based observations (e.g. the Composite Burn Index, CBI) have demonstrated the reliability of such remotely sensed indices within many ecosystems (Eidenshink et al., 2007; Hall et al., 2008; Soverel et al., 2010), precipitating extensive mapping efforts across the US and Canada. In the US, the Monitoring Trends and Burn Severity (MTBS; <https://www.mtbs.gov>) program has mapped satellite-inferred fire severity from 1984 to present for fires that are at least 2.02 (eastern US) or 4.04 (western US) km<sup>2</sup> in size (Picotte et al., 2020). In Canada, such data have also recently become available (Guindon et al., 2021; Whitman et al., 2020).

To date, these remotely sensed indices have shown mixed success in the boreal forest. Some studies found strong correlations between satellite-inferred severity metrics and the field-based measure of fire severity, CBI (Allen & Sorbel, 2008; Boucher et al., 2017; Epting et al., 2005; Hall et al., 2008; Rogers et al., 2014). Other studies have found weak correlations (Alonzo et al., 2017; Boby et al., 2010; Hoy et al., 2008; Murphy et al., 2008). Some of the challenges affecting the ability of satellite indices to accurately characterize field-measured severity of boreal fires include: intense productivity of post-fire colonizing plants, persistent cloud cover, saturation of spectral response at high fire severities, standing water in lowlands, downed trees with unburned canopies, low solar zenith angle, shadowing related to topography, and large variability in inter-annual vegetation phenology (Chen et al., 2020; French et al., 2008; Hoy et al., 2008; Verbyla et al., 2008). In addition, the commonly applied field method (CBI) has its own shortcoming for assessing fire severity in boreal forests, namely a limited ability to quantify organic layer consumption (Kasischke et al., 2008). Innovative approaches to solving these challenges are needed to improve the reliability and accuracy of satellite-inferred fire severity metrics in the North American boreal region.

Until recently, fire severity maps were commonly created by differencing individual Landsat scenes from before and after fire. The conventional method – called an ‘extended assessment’ (Key & Benson, 2006) – compares a Landsat scene generally taken from the growing season 1 year before fire to another scene from the growing season 1 year after fire. More recently, the cloud-computing platform Google Earth Engine has facilitated an entirely

new range of computing possibilities for satellite imagery applications (Gorelick et al., 2017). Earth Engine’s compute power and comprehensive data catalog allows for all images of interest within a date range to be quickly and easily analyzed on a pixel-wise basis and obviates the need for parsimonious data collections. As such, severity maps are no longer limited to single-scene Landsat comparisons; rather all clear pixels (i.e. without clouds, smoke, or shadows) across a date range of interest can be stacked, and a summary statistic (e.g. mean, median, minimum) calculated for each pixel in a stack (Guindon et al., 2021; Parks et al., 2018; Whitman et al., 2020). This approach, coined ‘compositing’, is increasingly applied to fires in the contiguous US (Parks et al., 2018, 2019; Souldard et al., 2016), Canada (Kato et al., 2020; Whitman et al., 2020), and much of the globe (Hislop et al., 2020; Pérez-Romero et al., 2019). The compositing approach is a faster method for assessing fire severity, as it does not rely on time-consuming a priori scene selection (Parks et al., 2018). It also allows for greater flexibility in selecting appropriate date ranges for pre- and post-fire imagery – an important feature for tailoring severity assessments to boreal ecosystems.

Leveraging the power of Earth Engine, we developed an alternative method for assessing fire severity in the North American boreal forest. Our approach, which we call a ‘hybrid composite’ method, modifies the conventional representation of the post-fire condition, that is, using imagery from the year following fire, and instead assembles all valid images between the immediate post-fire date and the early growing season of the following year. These images are composited to form a single image for the post-fire period. Our intention in modifying the post-fire time frame was to better incorporate the proximate effects directly after fire such as scorching, charring and mortality in the post-fire image, while minimizing the potential effects of intense plant colonization in the following year. Our main objective in this study is to demonstrate the hybrid composite method as an alternative remote sensing technique for evaluating fire severity in the boreal forests of North America. We compare the hybrid composite method to two versions of extended assessments (i.e. 1 year before vs. 1 year after): the ‘extended composite’, in which the pre- and post-fire images are represented by composites of the respective growing seasons (Parks et al., 2018; Whitman et al., 2020), and ‘paired-scene’, which relies on a single-date Landsat scene from each time period (Eidenshink et al., 2007; Key & Benson, 2006). We evaluate performances of each approach by modeling the relationships between satellite-inferred severity and the field-based measure of severity, CBI. We also provide Earth Engine code to produce gridded fire severity datasets using the hybrid composite approach.

## Materials and Methods

### Study Area

We focused our study on fires from forested areas of the boreal zone across Alaska and Canada (Brandt, 2009) for which we were able to acquire CBI data. Common tree species in the North American boreal forest include black spruce (*Picea mariana*), white spruce (*Picea glauca*), jack pine (*Pinus banksiana*), lodgepole pine (*Pinus contorta* var. *latifolia*), tamarack (*Larix laricina*), and broadleaf trees such as trembling aspen (*Populus tremuloides*), balsam poplar (*Populus balsamifera*), Alaska paper

birch (*Betula neoalaskana*), and paper birch (*Betula papyrifera*).

### Processing in Google Earth Engine

We used Earth Engine's capabilities to produce Landsat-based fire severity metrics for each of 52 fires from the boreal region (Fig. 1A; described further in Section 2.3). Fire severity metrics are based on the normalized burn ratio (NBR, Equation 1) and include: (a) delta normalized burn ratio (dNBR, Equation 2, Key & Benson, 2006), and (b) relativized burn ratio (RBR, Equation 3, Parks et al., 2014), as follows:

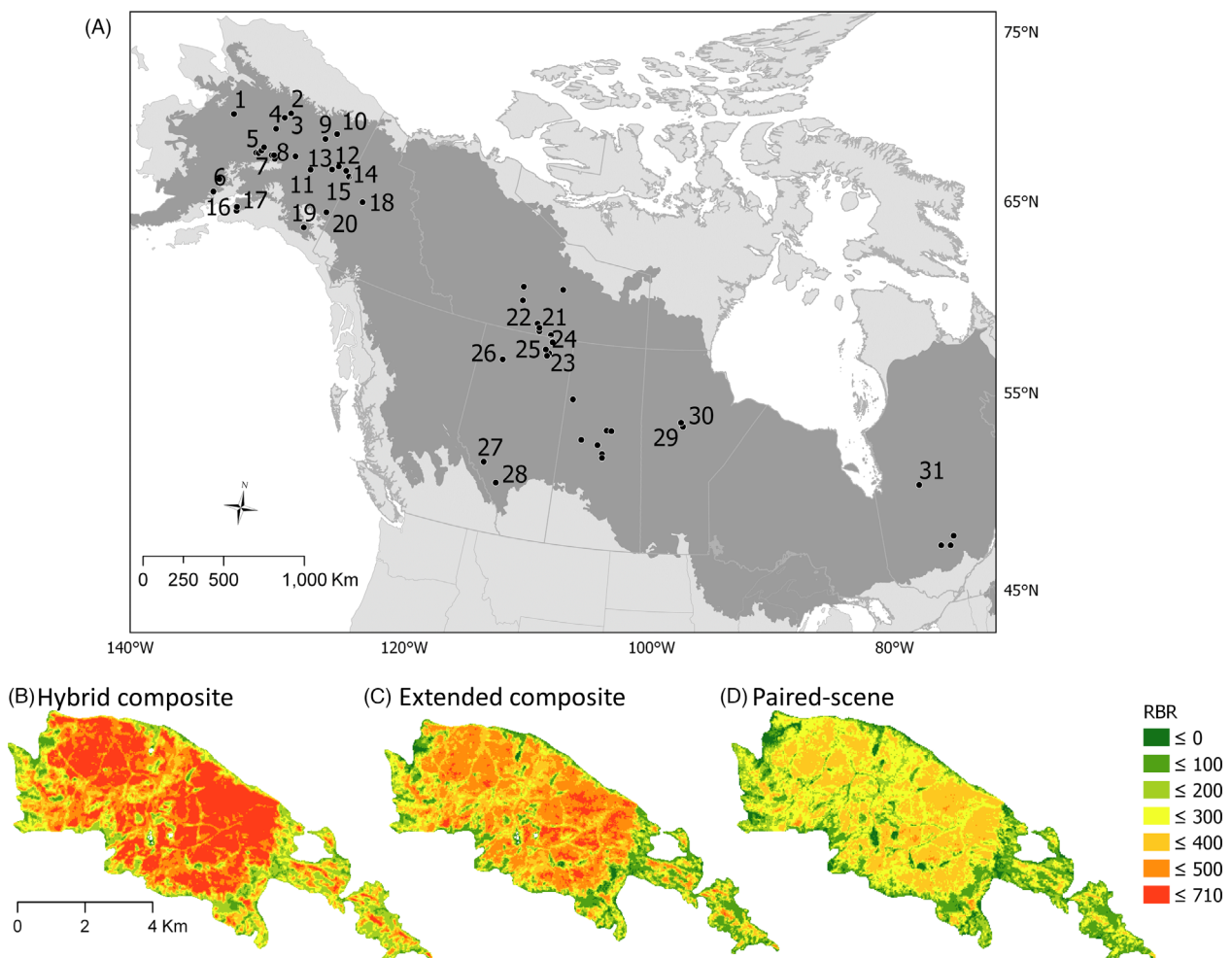


**Figure 1.** Locations (A) of the 52 fires included in the validation of the delta normalized burn ratio (dNBR) and relativized burn ratio (RBR). North American boreal zone is shown in dark gray shading. Numeric labels indicate locations of fires with at least 25 CBI plots (see Table 3) as follows: (1) Bonanza Creek, (2) Clawanmenka Lake, (3) Old Dummy, (4) Tanana Area, (5) Herron River, (6) Currant Creek, (7) Chitsia, (8) Survey Line, (9) Lower Mouth, (10) Winter Trail, (11) Delta Complex, (12) Beverly, (13) Andrew Creek, (14) Witch, (15) Jessica, (16) Funny River, (17) Glacier Creek, (18) Dawson, (19) Chakina, (20) Black Hill, (21) Angus Pine 1, (22) Sandy, (23) Jordn Creek, (24) Peace Point #1, (25) Lake One, (26) Chuckegg, (27) Southesk, (28) Dogrib, (29) Thompson Lake, (30) Burntwood, and (31) 2013080250. Example visualization of RBR for the Andrew Creek fire using: (B) the hybrid composite, (C) extended composite, and (D) paired scene methods.

$$\text{NBR} = \left( \frac{\text{NIR} - \text{SWIR}}{\text{NIR} + \text{SWIR}} \right) \quad (1)$$

$$\text{dNBR} = (\text{NBR}_{\text{prefire}} - \text{NBR}_{\text{postfire}}) \times 1000 \quad (2)$$

$$\text{RBR} = \frac{\text{dNBR}}{\text{NBR}_{\text{prefire}} + 1.001} \quad (3)$$

where NIR and SWIR in equation 1 are the near infrared and shortwave infrared bands respectively (White et al., 1996). NIR usually declines after fire due to vegetation mortality and char deposition, whereas SWIR increases due to greater soil exposure, char and moisture loss in the overstory and understory (Bright et al., 2019).

In Earth Engine, we implemented the compositing approach (Parks et al., 2018; Whitman et al., 2020), where a mean for each pixel is taken across a stack of images that occur within a given date range. We explored other metrics (e.g. minimum, median) for summarizing NBR and found the best results using a ‘mean’ for the image reduction process. We used Landsat Surface Reflectance Tier 1 datasets, including TM, ETM+, and OLI imagery, and selected the set of best-available data by removing any pixels with snow, clouds, shadow, or water, based on the quality assessment band in each image.

We tested two different scenarios for ranges of dates used to create post-fire NBR to evaluate the potential for improvements in fire severity metrics with compositing methods (Table 1). For the hybrid composite approach (Fig. 2), the post-fire NBR image included dates from immediately after the fire was extinguished through 15 November of that year, plus dates from the following year starting when snow cover was absent from the fire perimeter through 1 July. Any pixels selected within this time period that had snow (e.g. in early November) were excluded from the imagery dataset based on the quality assessment band. For fires occurring in years 2000 onward, we used data products from the Moderate

Resolution Imaging Spectroradiometer (MODIS) sensors to determine the dates when each fire was extinguished and when the spring snow-free period started (Fig. 2). MODIS sensors provide higher temporal resolution than Landsat (i.e. daily vs. ~16 day repeat cycle; Goward et al., 2017) but lower spatial resolution (1-km vs. 30-m). The daily frequency of MODIS allowed us to pinpoint appropriate dates for the post-fire imagery but the difference in spatial resolution between MODIS and Landsat necessitated that we determine fire termination and snow-free dates across whole fires rather than on a per-pixel basis. Specifically, we used MODIS Terra and Aqua Thermal Anomalies and Fire Daily Global datasets (MOD14A1 V6 and MYD14A1 V6, respectively) to assess the date when burned pixels no longer occurred within a fire perimeter. In the year following fire, we used MODIS Terra and Aqua Snow Cover Daily Global datasets (MOD10A1 V6 and MYD10A1 V6, respectively) to identify when snow cover no longer existed within a fire perimeter. Here, we queried the earliest day from late winter to summer (i.e. 1 February to 1 July) when snow cover was 5% or less for each pixel, and then selected the 95<sup>th</sup> and 75<sup>th</sup> percentile values across each fire. The snowmelt day for the fire was assigned to the 95<sup>th</sup> percentile value if that day occurred before 1 July, otherwise the 75<sup>th</sup> percentile was used; if the 75<sup>th</sup> percentile value occurred after 1 July, we assumed 30 April as the snowmelt day for the fire. MODIS imagery became available in 2000, but the data coverage may be constrained due to outages (e.g. 6–8 August 2000 and 16 June to 2 July 2001; Giglio et al., 2013) or cloud cover (Ziel et al., 2020). Where MODIS data coverage was limited, we assumed that fires were extinguished by 15 September for the year of fire and snowmelt completed by 30 April for the year following fire, with the exception of the late-season Dogrib fire which terminated on 21 October 2001 (Boychuk et al., 2009). For the extended composite approach, post-fire NBR imagery was created by compositing pixels from the fire season date range (20 May–31 August, Table 1) from 1 year after fire; this time period reflects the general time-frame in which a single scene would typically be selected in a paired-scene assessment.

For both the hybrid and extended assessment composites, the pre-fire image date range was 20 May to 31 August (Table 1) to reflect the typical fire season (Abatzoglou & Kolden, 2011; Stocks et al., 2002) and vegetation conditions during the summer growing season in the North American boreal zone. We acknowledge that the range of dates that best represent fire severity and phenological patterns varies annually, but by computing a time-integrated mean, we aimed to capture the dominant signal in NBR across each time period.

**Table 1.** Image season date ranges for composite methods to develop and evaluate fire severity metrics.

Method type	Pre-fire NBR		Post-fire NBR	
	Start	End	Start	End
Extended	May 20	Aug 31	May 20 YAF	Aug 31 YAF
Hybrid	May 20	Aug 31	Day after fire ends YOF	Nov 15 YOF
	YBF	YBF	Day after snow cover ends YAF	Jul 1 YAF

Start/end columns indicate the dates within which imagery was included for calculating NBR. YBF, year before fire; YAF, year after fire; YOF, year of fire; NBR, normalized burn ratio.

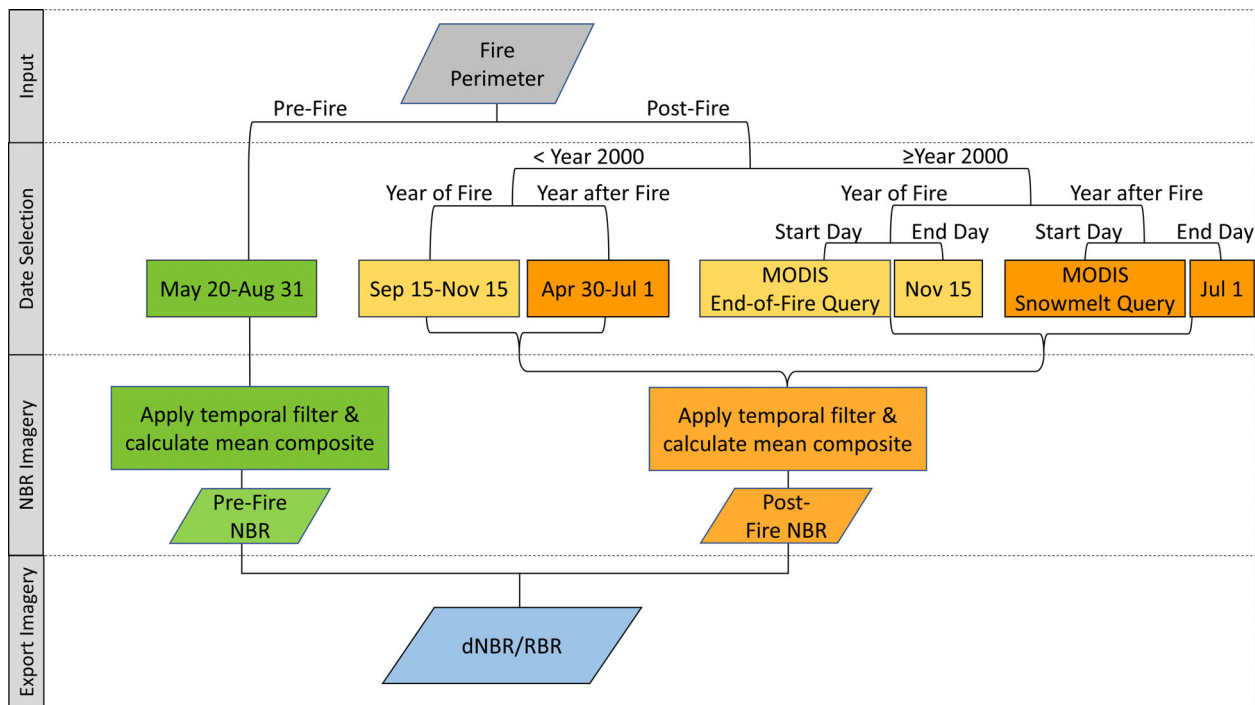


**Figure 2.** Flowchart describing the process to create Landsat-derived fire severity metrics in Google Earth Engine using the hybrid composite approach. Parallelograms represent data types, and rectangles indicate processing selections or steps.

**Evaluation**

We compared dNBR and RBR produced using hybrid compositing, extended compositing and paired scenes. For the paired-scene method, we acquired pre- and post-fire imagery from the MTBS program (mtbs.gov) for fires in the US. For Canada, we identified paired pre- and post-fire Landsat scenes with minimal cloud, shadow or snow for each fire, and produced fire severity metrics using Earth Engine.

Our evaluations were based on the correspondence of dNBR and RBR to the field-based, continuous measure of severity, CBI (Key & Benson, 2006). The CBI method visually assesses fire effects across five forest strata (i.e. substrate; herbs, low shrubs, saplings; tall shrubs and small trees; intermediate trees; big trees) by evaluating factors such as surface fuel consumption, soil char, vegetation mortality and scorching of trees (Key & Benson, 2006). CBI values range from 0 to 3, with 0 being unburned and 3 representing the most severe burn. At each CBI plot location, we extracted satellite-derived dNBR and RBR values using bilinear interpolation. A number of fires lacked CBI plots representing unburned or very low severity, which are important in building balanced regression models (Parks et al., 2019). Similar to Parks et al. (2019), we supplemented our plot dataset,

where needed, such that each fire had at least 10% of its plots represented by CBI  $\leq 0.25$ . These additional ‘pseudo-plots’ were created for 15 fires by randomly selecting unburned pixels at a distance of 200 m outside fire perimeters in areas that were not composed of rock or water; these plots were assigned a CBI value of 0. In total, we gathered CBI data for 52 fires, 24 in Alaska and 28 in Canada. The initial number of CBI plots varied for each method because the availability of cloud-, shadow-, and snow-free pixels varied. We selected plots with valid imagery (i.e. clear) and common to the hybrid and extended composite and paired-scene approaches to ensure a common dataset (1788 plots in total) was available to consistently compare results across methods.

We evaluated each satellite-inferred severity metric using non-linear least-squares (NLS) regression models with CBI as the dependent variable using plot data from all 52 fires combined. We used a fivefold cross-validation; for each of the fivefolds, we used 80% of the data to train the model and the remaining 20% for testing (i.e. we used the model to predict CBI). The non-linear regression equation was, as follows:

$$CBI = a \times (1 - \exp(-b \times y)) \tag{4}$$

where  $y$  was the satellite-derived metric being evaluated and starting values for  $a$  and  $b$  in the algorithm were 3.2

and 0.002 respectively. Least-square regression modeling was performed using R software and implementing the NLS function (R Development Core Team, 2021). We built three models for each approach and fire severity metric, one with Alaskan and Canadian fires combined and individual models for Alaska and Canada. Following Whitman et al. (2020), predictions outside the range of field measurements (0–3) were curtailed to the field-observed range. We tested model skill by comparing observed and predicted CBI using linear regression for each severity metric, reporting the coefficient of determination (i.e.  $R^2$  of linear regression), root-mean-square error (RMSE) as a measure of model spread, and mean absolute error (MAE) as a measure of bias. Availability of Landsat imagery began consistently increasing in boreal regions in 2001 with both Landsat 5 and 7 satellites operational (note, Landsat 7 was launched in 1999 nearly doubling image availability but Landsat 5 TM acquisition declined markedly for 1 year in 2000 in boreal regions, cf. Sulla-Menashe et al., 2016); correspondingly, satellite measures of burn severity improved with the greater image availability (Chen et al., 2021). Therefore, we also included analyses restricted to fires from the 2002–2019 time period, such that all pre- and post-fire imagery were acquired from 2001 onward. That is, we constrained validation statistics into two time periods, fires that occurred during 1999–2019 and 2002–2019, for each of the three sets of models.

Using the NLS model that included both Alaska and Canada (years 1999–2019) with predictions based on a fivefold cross validation, we also produced validation statistics on a per-fire basis to examine whether fire severity methods performed better for certain fires or fire years. For these per-fire comparisons, we only selected fires with at least 25 CBI plots (not including pseudo-plots previously described) to ensure model validations were adequately robust. There were 31 fires meeting our criteria (12 in Canada, 19 in Alaska; Fig. 1A).

Thresholds were also developed to categorize satellite-inferred severity data into low-, moderate-, and high-severity classes. We identified these thresholds using the NLS regression models described above, except that we applied models across the entire CBI dataset (1788 plots) rather than with a cross-validated approach. Accordingly, we used the models to, first, predict CBI across a range of values representing satellite-inferred severity (0–1000). We then identified the satellite-derived severity values that correspond to predicted CBI, at values which are well-recognized as representing breaks for classifying field-derived severity, as follows: 0–1.24 for low severity, 1.25–2.25 for moderate severity, and 2.26–3.0 for high severity (Miller & Thode, 2007). These thresholds were developed for both dNBR and RBR for each composite method and

the paired-scene method for fires across all years, in Alaska and Canada combined and separately.

Lastly, we counted the number of scenes contributing to each pre- and post-fire image, calculated statistical summaries for each composite method, and evaluated relationships between the number of scenes in post-fire images and  $R^2$  between CBI predicted versus observed (i.e. performance) on a per-fire basis.

## Results

The hybrid composite approach generally outperformed (higher  $R^2$ , lower RMSE error, and lower MAE bias) other approaches in measuring fire severity (Table 2). The

**Table 2.** Model fit ( $R^2$ ), root-mean-square error (RMSE) and mean absolute error (MAE) for non-linear least-squares regression models predicting Composite Burn Index (CBI) from burn severity metrics of the differenced normalized burn ratio (dNBR) and relativized burn ratio (RBR) produced from the hybrid and extended composite methods, and paired-scene method.

Severity metric & method	1999–2019			2002–2019		
	$R^2$	RMSE	MAE	$R^2$	RMSE	MAE
Alaska & Canada						
dNBR: hybrid composite	0.70	0.40	0.32	0.72	0.39	0.31
dNBR: extended composite	0.66	0.47	0.37	0.68	0.45	0.35
dNBR: paired-scene	0.64	0.51	0.40	0.66	0.48	0.38
RBR: hybrid composite	0.71	0.40	0.32	0.73	0.39	0.31
RBR: extended composite	0.66	0.49	0.38	0.68	0.47	0.37
RBR: paired-scene	0.63	0.52	0.41	0.65	0.50	0.40
Alaska						
dNBR: hybrid composite	0.65	0.41	0.33	0.72	0.38	0.30
dNBR: extended composite	0.61	0.51	0.39	0.66	0.47	0.36
dNBR: paired-scene	0.60	0.50	0.39	0.66	0.43	0.34
RBR: hybrid composite	0.67	0.41	0.32	0.73	0.38	0.30
RBR: extended composite	0.61	0.52	0.40	0.66	0.48	0.37
RBR: paired-scene	0.60	0.51	0.41	0.65	0.45	0.36
Canada						
dNBR: hybrid composite	0.74	0.39	0.31	0.73	0.39	0.31
dNBR: extended composite	0.72	0.43	0.34	0.71	0.44	0.35
dNBR: paired-scene	0.69	0.50	0.40	0.68	0.51	0.41
RBR: hybrid composite	0.75	0.39	0.31	0.74	0.40	0.31
RBR: extended composite	0.71	0.45	0.36	0.69	0.46	0.36
RBR: paired-scene	0.69	0.50	0.40	0.68	0.51	0.41

Results from each metric and method are presented for Alaska and Canada combined and separately across all available fire years (1999–2019) and for the subset of 2002–2019.

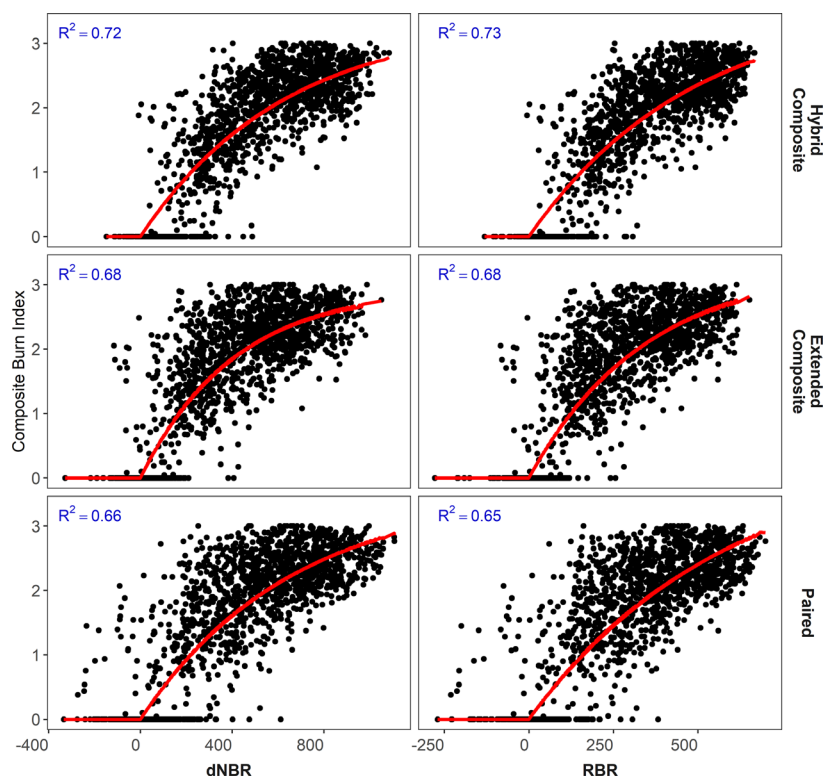


**Figure 3.** Non-linear least-squares regression models of the field-based Composite Burn Index as a function of dNBR and RBR severity metrics for the hybrid and extended composite methods, and the paired-scene method for fires from 2002 to 2019 in the boreal region of Alaska and Canada. Red lines are the modeled fit of regressions, and the resulting  $R^2$  is shown in blue.

elevated performance was evident across nearly all areas, time periods, and severity metrics. In Alaska, the  $R^2$  of predicted versus observed CBI for the hybrid approach was consistently higher than the next-best method across all metrics, methods, and time periods (Table 2; Fig. S1). In Canada, the hybrid composite also performed better across metrics, methods, and time periods, particularly with the RBR metric (Table 2; Fig. S2). Considering both countries combined, the hybrid composite method again outperformed other methods across metrics, methods, and time periods (Table 2; Fig. 3).

All three methods generally performed better, on a per-fire basis, from 2002 onward compared to previous years, with the hybrid composite method demonstrating the most consistently high model fits. On average,  $R^2$  values from modeling fires using the hybrid composite method were  $>0.70$  across Alaska and Canada, with a handful of exceptions in 2004, 2014, and 2019 (Table 3). Two fires (Clawanmenka Lake 2004 in Alaska and Chuckegg 2019 fire in Canada) showed relatively lower  $R^2$  values (0.45–0.66) across all severity metrics and methods. The 2014 Funny River fire (Alaska) also performed relatively poorly across all metrics and methods ( $R^2$  values of 0.39–0.66),

except for the paired-scene method ( $R^2$  values of 0.91–0.92), which in this case, the MTBS program used a post-fire scene from the year of fire rather than the conventional timing of the year following fire. In addition, the correspondence between CBI and each of the severity metrics of dNBR and RBR was very comparable across all time periods and areas. Lastly, for demonstration purposes, we present example maps of dNBR produced using each of the three methods for one fire – 2018 Andrew Creek in Alaska (Fig. 1B–D).

Thresholds for classifying satellite-inferred severity data into low-, moderate-, and high-severity classes are shown in Table 4. These thresholds may be applied to severity products created for fires in this study, or practitioners can implement the compositing or paired-scene methods to other fires and classify the resulting datasets with these threshold values.

For the composite methods, the number of scenes contributing to pre-fire imagery averaged  $7.9 (\pm 4.4 \text{ SD})$  across all boreal fires, whereas post-fire imagery averaged  $9.9 (\pm 4.1 \text{ SD})$  and  $11.9 (\pm 5.9 \text{ SD})$  for extended and hybrid assessments respectively (Table S1). We found positive relationships between the number of scenes (contributing

**Table 3.**  $R^2$  from model fits relating CBI to severity metrics on a per-fire basis for the hybrid and extended composite methods and the paired-scene method, where the first value under each method is  $R^2$  for dNBR and the second value is  $R^2$  for RBR.

Fire name	Fire year	Region	Hybrid composite		Extended composite		Paired-scene		Number of plots
			dNBR	RBR	dNBR	RBR	dNBR	RBR	
Beverly	1999	AK	0.64	0.68	0.63	0.65	0.56	0.57	40
Jessica	1999	AK	0.68	0.66	0.70	0.69	0.61	0.60	47
Witch	1999	AK	0.71	0.76	0.63	0.69	0.86	0.84	32
Chitsia	2000	AK	0.81	0.82	0.82	0.84	0.87	0.86	25
Dogrib	2001	CAN	0.79	0.83	0.74	0.78	0.71	0.76	50
Herron River	2001	AK	0.86	0.87	0.86	0.86	0.82	0.81	25
Survey Line	2001	AK	0.57	0.60	0.48	0.49	0.48	0.50	87
Burntwood	2003	CAN	0.92	0.91	0.91	0.91	0.93	0.93	26
Thompson Lake	2003	CAN	0.77	0.78	0.83	0.84	0.77	0.78	56
Black Hill	2003	AK	0.85	0.84	0.82	0.80	0.87	0.85	65
Angus Pine 1	2004	CAN	0.84	0.84	0.89	0.89	0.90	0.89	70
Dawson	2004	CAN	0.90	0.90	0.86	0.86	0.80	0.80	37
Glacier Creek	2004	AK	0.89	0.91	0.85	0.85	0.85	0.87	39
Bonanza Creek	2004	AK	0.81	0.82	0.82	0.82	0.76	0.75	64
Lower Mouth	2004	AK	0.74	0.75	0.65	0.65	0.74	0.74	53
Clawanmenka Lake	2004	AK	0.66	0.63	0.56	0.52	0.52	0.47	70
Winter Trail	2004	AK	0.91	0.90	0.92	0.91	0.93	0.91	50
Old Dummy	2005	AK	0.73	0.72	0.70	0.69	0.54	0.53	63
Peace Point #1	2005	CAN	0.85	0.85	0.91	0.92	0.92	0.92	47
Southesk	2006	CAN	0.77	0.76	0.81	0.82	0.78	0.79	44
Lake One	2007	CAN	0.77	0.78	0.74	0.74	0.63	0.63	59
Jordin Creek	2007	CAN	0.79	0.79	0.71	0.71	0.68	0.70	43
Sandy	2008	CAN	0.86	0.87	0.80	0.81	0.80	0.82	100
Chakina	2009	AK	0.81	0.82	0.84	0.85	0.35	0.37	66
Delta Complex	2010	AK	0.94	0.95	0.88	0.90	0.87	0.88	30
20131080250	2013	CAN	0.82	0.84	0.85	0.87	0.84	0.85	44
Currant Creek	2013	AK	0.80	0.80	0.84	0.85	0.86	0.87	43
Funny River	2014	AK	0.66	0.66	0.40	0.39	0.92	0.91	49
Tanana Area	2015	AK	0.82	0.83	0.81	0.82	0.88	0.88	38
Andrew Creek	2018	AK	0.90	0.87	0.87	0.85	0.80	0.79	28
Chuckegg	2019	CAN	0.56	0.57	0.65	0.62	0.45	0.48	46

Only fires with at least 25 CBI plots were selected to ensure robust model validation. CBI, Composite Burn Index; dNBR, differenced normalized burn ratio; RBR, relativized burn ratio; AK, Alaska; CAN, Canada.

to post-fire imagery) and the performance of fires (i.e.  $R^2$  from CBI predicted vs. observed) across metrics for the hybrid composite method ( $r = 0.4$  for dNBR,  $r = 0.37$  for RBR;  $P < 0.05$  for both metrics), while the extended composite method showed weak relationships ( $r = -0.01$  and  $P = 0.97$  for dNBR,  $r = -0.1$  and  $P = -0.59$  for RBR).

## Discussion

The hybrid composite approach, which composites imagery from immediately after a fire and from the following spring and early summer, demonstrates the most promise for improving satellite-derived fire severity estimates in North American boreal forests. This approach uses a

relatively novel process of querying MODIS data to inform dates of appropriate Landsat image selection (cf. Hislop et al., 2020); that is, MODIS queries inform the date a fire was extinguished and date of snowmelt the following spring which in turn determines Landsat imagery selection. The proposed hybrid composite method improves the relationship between satellite-derived and on-the-ground metrics of severity by circumventing some of the challenges associated with fire severity mapping of high-latitude forests. The hybrid composite method takes advantage of new remote sensing technology, a large collection of CBI plots, and a growing understanding of fire severity in the boreal forest of North America. As such, it represents the next step in the evolution of fire-severity mapping for this ecosystem.



**Table 4.** Threshold values for each fire severity metric corresponding to low (CBI = 0–1.24), moderate (CBI = 1.25–2.25), and high severity (CBI = 2.26–3) produced from hybrid and extended composite methods, and paired-scene method.

	dNBR			RBR		
	Low	Moderate	High	Low	Moderate	High
Alaska & Canada						
Hybrid composite	≤289	290–690	≥691	≤201	202–461	≥462
Extended composite	≤223	224–583	≥584	≤164	165–394	≥395
Paired-scene	≤286	287–667	≥668	≤207	208–450	≥451
Alaska						
Hybrid composite	≤285	286–697	≥698	≤200	201–466	≥467
Extended composite	≤223	224–591	≥592	≤165	166–398	≥399
Paired-scene	≤247	248–645	≥646	≤176	177–422	≥423
Canada						
Hybrid composite	≤292	293–683	≥684	≤202	203–456	≥457
Extended composite	≤223	224–573	≥574	≤162	163–389	≥390
Paired-scene	≤328	329–685	≥686	≤245	246–476	≥477

Results from each metric and method are presented for Alaska and Canada combined and separately across all fire years (1999–2019). CBI, Composite Burn Index; dNBR, differenced normalized burn ratio; RBR, relativized burn ratio.

The higher performance of the hybrid composite method is likely related to its ability to capture the initial and longer term effects of fire, while moderating seasonal factors that obscure spectral response measures related to fire effects. Fires in the North American boreal forest often burn as high-intensity, crown fires that kill most of the overstory and understory vegetation (Kasischke et al., 2008; Viereck, 1983). In the year following fire, understory species rapidly regenerate (Hart & Chen, 2006) with communities dominated by fast-growing vascular plants (Greene et al., 1999), although non-vascular species may represent a significant component of the recolonization as well (Pinno & Errington, 2016; Spellman et al., 2014). Revegetation can be rapid from rhizomatous re-sprouters in moderate and low-severity fires, whereas annual forbs and graminoid species can quickly colonize bare soil after high-severity burns (Hollingsworth et al., 2013; Pinno & Errington, 2016; Wang & Kembell, 2005). The hybrid composite method acquires and averages reflectance imagery starting from immediately after fire, and thus incorporates the immediate effects of fire, such as charring,

scorching, and under- and overstory mortality (Hudak et al., 2007), before vegetation recovery begins. In the year following fire, the hybrid composite method includes imagery from directly after snowmelt to early summer (1 July), and reduces the signal from the most intense peak of post-fire establishment of vegetation, which may affect severity–CBI relationships (Murphy et al., 2008). The extended method, in contrast, incorporates post-fire imagery through late summer, and more fully incorporates the prolific productivity from recolonization in the growing season after fire, which may more strongly disguise remote sensing measures of fire severity. The factors influencing spectral response measures of fire severity are complex (Murphy et al., 2008) and highly variable among ecosystems (French et al., 2008; Lentile et al., 2006), and it is thus challenging to disentangle their relative influences. However, the success demonstrated here indicates the potential for continued improvements by taking advantage of the image repository and cloud-computing environment provided by Earth Engine.

More generally, the hybrid composite method used here demonstrates that rapidly evolving technologies may help overcome certain challenges for using remote sensing to assess fire severity in northern latitudes. One challenge of the paired-scene approach is obtaining high-quality Landsat scenes with similar phenological timing (Chen et al., 2021). Cloud cover and smoke is a common issue for acquiring imagery in boreal regions, and cloud shadows can have greater effects due to low solar angle at high latitudes (Verbyla et al., 2008). Verbyla et al. (2008) reported variation in dNBR values attributable, in part, to varying seasonal timing of pre-fire scene acquisitions, which is often necessary due to limited availability of cloud-free scenes. In our study, one might have expected the paired-scene approach to outperform the extended composite approach because of greater precision by analysts in selecting pre- and post-fire scenes with similar timing (Whitman et al., 2020). However, in Alaska, these two methods had virtually identical performance, whereas in Canada, the extended composite approach performed slightly better than the paired-scene approach. We surmise that the ability to acquire cloud-free pixels more readily through image compositing can have equal if not more benefit to the challenges of analysts' selection of paired, cloud-free scenes. Not only is data quality on par with the paired-scene approach, but compositing methods provide an overall gain in the number of mapped pixels within burns due to the greater availability of pixels free of clouds and smoke (Whitman et al., 2020). Lastly, mean compositing approaches allow severity data to be, consistently, systematically, and easily produced, such that trends over time can be more reliably evaluated (Hislop et al., 2020).

On a fire-by-fire basis, the notable variation in validation statistics reflects the strengths and weaknesses of each approach. For fires burning early in the summer, such as the 2010 Delta Complex (Alaska) fire in the interior boreal zone, fire effects may be severe but some vegetation (such as forbs and grasses) can vigorously recover that summer. In these cases, the hybrid composite method better incorporates the severe fire effects that are evident immediately after fire. For fires where understory regrowth is relatively slow, such as the 2013 Currant Creek fire (Alaska; Barnes & Northway, 2015), the extended composite or paired-scene approaches may be more suitable, as they minimize variation from phenology and moisture content. Under the best of circumstances, when pre- and post-fire cloud-free scenes are available at narrowly similar times, the paired-scene approach may offer the best option as evidenced by the 2015 Tanana River fire (Alaska), where scene acquisition was exactly 1 year and 1 day apart and closely aligned to the fire anniversary date. Such variation highlights that the best approach for measuring fire severity may depend on the context and conditions of each fire, as well as the measurement objectives. If the goal is to monitor fire-induced ecological change and trends in a systematic way across fires, the hybrid composite method offers an improved and automated alternative for North American boreal forests.

A few fires demonstrated either varied or lower performances across methods, indicating the need for further improvements to remotely sensed measurements of fire severity in northern latitudes. One example is the 2014 Funny River fire on the Kenai Peninsula, Alaska, which ignited in May over frozen ground, prior to green-up, in a spruce-dominated-forest, where grass (mainly *Calamagrostis canadensis*) rapidly regenerated by mid-June of the following year (L. Saperstein, pers. comm.). The paired-scene approach ostensibly performed well compared to the compositing methods, but unlike all other paired-scene imagery obtained from MTBS, the post-fire Landsat scene for this fire was taken from immediately post-fire and thus, did not match the standard methodology used by MTBS in Alaska of extended assessments for paired-scene imagery (Picotte et al., 2020). A second example is the 2019 Chuckegg fire in the Canadian boreal plains in Alberta. This fire was dominated by deciduous (mainly trembling aspen) forest prior to burning and burned over several months. There was intense resprouting of aspen that same summer, while some parts of the fire were still burning. All CBI plots from the Chuckegg fire were in aspen-dominated stands. Corresponding model fits using the hybrid composite were better than expected (0.56–0.57), but still not on par with other fires from recent years; the extended composite and paired-scene methods

also showed weaker relationships (0.45–0.65; Table 2). Such incongruity in model fits across both spruce and deciduous forests demonstrates the need to incorporate tree-species dominance and site condition in remote sensing measures of fire severity.

Moving forward, the need for more refined remote sensing methods will only increase as climate change and fire catalyze forest conversion to different vegetation types (Coop et al., 2020; Stralberg et al., 2018). The boreal region of North America is warming twice as fast as the global average (Serreze & Barry, 2011). Rising temperatures have been associated with intensified fire weather, increased wildfire area burned, shorter fire intervals, and more severe fires (Veraverbeke et al., 2017; Whitman, Parisien, et al., 2019; Xiao & Zhuang, 2007). Interactions between climate change and fire are expected, for instance, to convert some black spruce forest to deciduous forest (Johnstone et al., 2010; Mekonnen et al., 2019; Searle & Chen, 2017), and indeed such transitions are already underway at regional scales in interior Alaska, and throughout the North American boreal biome (Hansen et al., 2020). Deciduous forests (e.g. aspen and birch) resprout prolifically after burning (de Groot & Wein, 1999; Johnstone, 2005), perhaps to an extent that strongly impacts surface reflectance and obscures remote sensing measures of fire severity. Our methods could be advanced by more precisely detecting the period of intense revegetation using other spectral measures highly sensitive to plant productivity, such as the Normalized Difference Vegetation Index (Nemani & Running, 1997), and thereby better identify imagery acquisition dates that precede regrowth in deciduous forests. Future research could also explore methods that downscale Landsat-derived NBR based on MODIS data to produce high temporal frequency and high spatial resolution severity measures (sensu Filgueiras et al., 2020).

## Conclusions

We present an alternative methodology, the ‘hybrid composite’, for producing fire severity metrics for the North American boreal region using freely available satellite data in the Earth Engine cloud-computing environment. This method offers an improvement over existing ones by more completely incorporating the range and variability of fire effects unique to the North American boreal zone. This approach can complement existing fire databases, and thereby broaden our understanding and monitoring of fire-induced change in boreal ecosystems. For instance, maps based on this method could help track potential effects on wildlife distribution from expected fire-related changes in plant communities, such as conversion from coniferous to deciduous forest following high-severity

fires (Russell & Johnson, 2019). Other ecosystems with rapid regrowth of burned vegetation, not only in boreal zones but the southeastern and southwestern United States (Picotte et al., 2020), may also benefit by applying similar methods that target the timing of Landsat sampling based on high temporal frequency MODIS data; however, plot data should be tested to evaluate the efficacy of the hybrid method to such ecosystems. Innovation in fire monitoring techniques is becoming increasingly important as area burned continues to increase with climate warming, and techniques such as the hybrid compositing method offer improve assessments of consequent fire effects in high-latitude ecosystems particularly sensitive to climate change.

## Acknowledgments

We extend our thanks to Michael Koontz and Zhigiang Yang for providing peer review of our Earth Engine code. We also gratefully acknowledge Jessica Walker and two anonymous reviewers for their review of this manuscript. This research was supported by the USDA Forest Service, Rocky Mountain Research Station, Aldo Leopold Wilderness Research Institute. The findings and conclusions in this publication are those of the authors and should not be construed to represent any official USDA or U.S. Government determination or policy. Any use of trade names is for descriptive purposes only and does not imply endorsement by the US Government.

## Code Availability

The code used to produce fire severity imagery for the Google Earth Engine hybrid composite method are available for use at this link: [https://code.earthengine.google.com/?scriptPath=users%2Fflisamholsinger%2Fboreal\\_hybrid\\_severity%3Amanuscript](https://code.earthengine.google.com/?scriptPath=users%2Fflisamholsinger%2Fboreal_hybrid_severity%3Amanuscript).

The code is set up to run on a subset (20) of the Alaskan and Canadian fires examined in this study and produces dNBR and RBR metrics.

## References

- Abatzoglou, J.T. & Kolden, C.A. (2011) Relative importance of weather and climate on wildfire growth in interior Alaska. *International Journal of Wildland Fire*, **20**(4), 479–486. <https://doi.org/10.1071/WF10046>
- Allen, J.L. & Sorbel, B. (2008) Assessing the differenced Normalized Burn Ratio's ability to map burn severity in the boreal forest and tundra ecosystems of Alaska's national parks. *International Journal of Wildland Fire*, **17**, 463–475.
- Alonzo, M., Morton, D.C., Cook, B.D., Andersen, H.-E., Babcock, C. & Pattison, R. (2017) Patterns of canopy and surface layer consumption in a boreal forest fire from repeat airborne lidar. *Environmental Research Letters*, **12**, 065004.
- Balshi, M.S., McGuire, A.D., Zhuang, Q., Melillo, J., Kicklighter, D.W., Kasichke, E. et al. (2007) The role of historical fire disturbance in the carbon dynamics of the pan-boreal region: a process-based analysis. *Journal of Geophysical Research: Biogeosciences*, **112**, 1–18. <https://doi.org/10.1029/2006JG000380>
- Barnes, J.L. & Northway, J.L. (2015) Alaska region fire ecology annual report for 2014. In Natural Resource Data Series, NPS/AKRO/NRDS-2015/781.
- Boby, L.A., Schuur, E.A.G., Mack, M.C., Verbyla, D. & Johnstone, J.F. (2010) Quantifying fire severity, carbon, and nitrogen emissions in Alaska's boreal forest. *Ecological Applications*, **20**(6), 1633–1647.
- Boucher, J., Beaudoin, A., Hebert, C., Guindon, L. & Bauce, E. (2017) Assessing the potential of the differenced Normalized Burn Ratio (dNBR) for estimating burn severity in eastern Canadian boreal forests. *International Journal of Wildland Fire*, **26**(2004), 32–45.
- Boyчук, D., Braun, W.J., Kulperger, R.J., Krougly, Z.L. & Stanford, D.A. (2009) A stochastic forest fire growth model. *Environmental and Ecological Statistics*, **16**(2), 133–151. <https://doi.org/10.1007/s10651-007-0079-z>
- Brandt, J.P. (2009) The extent of the North American boreal zone. *Environmental Research Letters*, **17**, 101–161. <https://doi.org/10.1139/A09-004>
- Bright, B.C., Hudak, A.T., Kennedy, R.E., Braaten, J.D. & Henareh Khalyani, A. (2019) Examining post-fire vegetation recovery with Landsat time series analysis in three western North American forest types. *Fire Ecology*, **15**, 8. <https://doi.org/10.1186/s42408-018-0021-9>
- Chen, D., Fu, C., Hall, J.V., Hoy, E.E. & Loboda, T.V. (2021) Spatio-temporal patterns of optimal Landsat data for burn severity index calculations: implications for high northern latitudes wildfire research. *Remote Sensing of Environment*, **258**, 112393. <https://doi.org/10.1016/j.rse.2021.112393>
- Chen, D., Loboda, T.V. & Hall, J.V. (2020). A systematic evaluation of influence of image selection process on remote sensing-based burn severity indices in North American boreal forest and tundra ecosystems. *Journal of Photogrammetry and Remote Sensing*, **159**(November 2019), 63–77. <https://doi.org/10.1016/j.isprsjprs.2019.11.011>
- Coop, J.D., Parks, S.A., Stevens-Rumann, C.S., Crausbay, S.D., Higuera, P.E., Hurteau, M.D. et al. (2020) Wildfire-driven forest conversion in western North American landscapes. *BioScience*, **70**(8), 659–673. <https://doi.org/10.1093/biosci/biaa061>
- de Groot, W.J. & Wein, R.W. (1999) *Betula glandulosa* Michx. response to burning and postfire growth temperature and implications of climate change. *International Journal of Wildland Fire*, **9**(1), 51–64.
- Duffy, P.A., Epting, J., Graham, J.M., Rupp, T.S. & McGuire, A.D. (2007) Analysis of Alaskan burn severity patterns using

- remotely sensed data. *International Journal of Wildland Fire*, **16**, 277–284. <https://doi.org/10.1071/WF06034>
- Eidenshink, J.C., Schwind, B., Brewer, K., Zhu, Z.-L., Quayle, B. & Howard, S.M. (2007) A project for monitoring trends in burn severity. *Fire Ecology*, **3**(1), 3–21.
- Epting, J., Verbyla, D. & Sorbel, B. (2005) Evaluation of remotely sensed indices for assessing burn severity in interior Alaska using Landsat TM and ETM+. *Remote Sensing of Environment*, **96**, 328–339. <https://doi.org/10.1016/j.rse.2005.03.002>
- Filgueiras, R., Mantovani, E.C., Fernandes-Filho, E.I., da Cunha, F.F., Althoff, D. & Dias, S.H.B. (2020) Fusion of MODIS and Landsat-like images for daily high spatial resolution NDVI. *Remote Sensing*, **12**, 1297. <https://doi.org/10.3390/RS12081297>
- French, N.H.F., Kasischke, E.S., Hall, R.J., Murphy, K.A., Verbyla, D.L., Hoy, E.E. et al. (2008) Using Landsat data to assess fire and burn severity in the North American boreal forest region: an overview and summary of results. *International Journal of Wildland Fire*, **17**, 443–462.
- Giglio, L., Randerson, J.T. & Van Der Werf, G.R. (2013) Analysis of daily, monthly, and annual burned area using the fourth-generation global fire emissions database (GFED4). *Journal of Geophysical Research: Biogeosciences*, **118** (1), 317–328. <https://doi.org/10.1002/jgrg.20042>
- Gorelick, N., Hancher, M., Dixon, M., Ilyushchenko, S., Thau, D. & Moore, R. (2017) Google Earth Engine: Planetary-scale geospatial analysis for everyone. *Remote Sensing of Environment*, **202**, 18–27. <https://doi.org/10.1016/j.rse.2017.06.031>
- Goward, S., Williams, D., Arvidson, T., Rocchio, L., Irons, J., Russell, C. et al. (2017) *Landsat's enduring legacy: pioneering global land observations from space*. Bethesda, MD: American Society for Photogrammetry and Remote Sensing.
- Greene, D.F., Zasada, J.C., Sirois, L., Kneeshaw, D., Morin, H., Charron, I. et al. (1999) A review of the regeneration dynamics of North American boreal forest tree species. *Canadian Journal of Forest Research*, **29**, 824–839.
- Guindon, L., Gauthier, S., Manka, F., Parisien, M.-A., Whitman, E., Bernier, P. et al. (2021) Trends in wildfire burn severity across Canada, 1985 to 2015. *Canadian Journal of Forest Research*, **51**(9), 1–43.
- Hall, R.J.A., Freeburn, J.T.A., de Groot, W.J., Pritchard, J.M.A., Lynham, T.J.B. & Landry, R.C. (2008). Remote sensing of burn severity: experience from western Canada boreal fires. *International Journal of Wildland Fire*, **17** (November 2006), 476–489.
- Hansen, W.D., Fitzsimmons, R., Olnes, J. & Williams, A.P. (2020) An alternate vegetation type proves resilient and persists for decades following forest conversion in the North American boreal biome. *Journal of Ecology*, **May**, 1–14. <https://doi.org/10.1111/1365-2745.13446>
- Hart, S.A. & Chen, H.Y.H. (2006) Understorey vegetation dynamics of North American boreal forests. *Critical Reviews in Plant Sciences*, **25**(4), 381–397. <https://doi.org/10.1080/07352680600819286>
- Hawbaker, T.J., Vanderhoof, M.K., Beal, Y.J., Takacs, J.D., Schmidt, G.L., Falgout, J.T. et al. (2017) Mapping burned areas using dense time-series of Landsat data. *Remote Sensing of Environment*, **198**, 504–522. <https://doi.org/10.1016/j.rse.2017.06.027>
- Hislop, S., Haywood, A., Jones, S., Soto-Berelov, M., Skidmore, A. & Nguyen, T.H. (2020). A satellite data driven approach to monitoring and reporting fire disturbance and recovery across boreal and temperate forests. *International Journal of Applied Earth Observation and Geoinformation*, **87** (October 2019), 102034. <https://doi.org/10.1016/j.jag.2019.102034>
- Hollingsworth, T.N., Johnstone, J.F., Bernhardt, E.L. & Chapin, F.S. (2013) Fire severity filters regeneration traits to shape community assembly in Alaska's boreal forest. *PLoS One*, **8**(2), e56033. <https://doi.org/10.1371/journal.pone.0056033>
- Hoy, E.E., French, N.H.F., Turetsky, M.R., Trigg, S.N. & Kasischke, E.S. (2008) Evaluating the potential of Landsat TM / ETM + imagery for assessing fire severity in Alaskan black spruce forests. *International Journal of Wildland Fire*, **17**, 500–514.
- Hudak, A.T., Morgan, P., Bobbitt, M.J., Smith, A.M.S., Lewis, S.A., Lentile, L.B. et al. (2007) The relationship of multispectral satellite imagery to immediate fire effects. *Fire Ecology*, **3**(1), 64–90.
- Johnstone, J.F. (2005) Effects of aspen (*Populus tremuloides*) sucker removal on postfire conifer regeneration in central Alaska. *Canadian Journal of Forest Research*, **35**, 483–486. <https://doi.org/10.1139/X04-171>
- Johnstone, J.F., Hollingsworth, T.N., Chapin, F.S. III & Mack, M.C. (2010) Changes in fire regime break the legacy lock on successional trajectories in Alaskan boreal forest. *Global Change Biology*, **16**, 1281–1295. <https://doi.org/10.1111/j.1365-2486.2009.02051.x>
- Kasischke, E.S., Turetsky, M.R., Ottmar, R.D., French, N.H.F., Hoy, E.E. & Kane, E.S. (2008) Evaluation of the composite burn index for assessing fire severity in Alaskan black spruce forests. *International Journal of Wildland Fire*, **17**(2006), 515–526.
- Kasischke, E.S., Verbyla, D.L., Rupp, T.S., McGuire, A.D., Murphy, K.A., Jandt, R. et al. (2010) Alaska's changing fire regime — implications for the vulnerability of its boreal forests. *Canadian Journal of Forest Research*, **40**, 1313–1324. <https://doi.org/10.1139/X10-098>
- Kato, A., Thau, D., Hudak, A.T., Meigs, G.W. & Moskal, L.M. (2020). Quantifying fire trends in boreal forests with Landsat time series and self-organized criticality. *Remote Sensing of Environment*, **237**(April 2019), 111525. <https://doi.org/10.1016/j.rse.2019.111525>
- Key, C.H. & Benson, N.C. (2006) Landscape assessment (LA). In: Lutes, D., Keane, R.E., Caratti, J.F., Key, C.H., Benson,

- N.C., Sutherland, S. & Gangi, L. (Eds.) *FIREMON: fire effects monitoring and inventory system*. Gen. Tech. Rep. RMRS-GTR-164-CD. Fort Collins, CO: USDA Forest Service, Rocky Mountain Research Station, pp. 1–55.
- Kolden, C.A. & Rogan, J. (2013) Mapping wildfire burn severity in the Arctic tundra from downsampled MODIS data. *Arctic, Antarctic, and Alpine Research*, **45**(1), 64–76. <https://doi.org/10.1657/1938-4246-45.1.64>
- Lentile, L.B., Holden, Z.A., Smith, A.M.S., Falkowski, M.J., Hudak, A.T., Morgan, P. et al. (2006) Remote sensing techniques to assess active fire characteristics and post-fire effects. *International Journal of Wildland Fire*, **15**, 319–345. <https://doi.org/10.1071/WF05097>
- Mekonnen, Z.A., Riley, W.J., Randerson, J.T., Grant, R.F. & Rogers, B.M. (2019) Expansion of high-latitude deciduous forests driven by interactions between climate warming and fire. *Nature Plants*, **5**(9), 952–958. <https://doi.org/10.1038/s41477-019-0495-8>
- Miller, J.D. & Thode, A.E. (2007) Quantifying burn severity in a heterogeneous landscape with a relative version of the delta Normalized Burn Ratio (dNBR). *Remote Sensing of Environment*, **109**(1), 66–80. <https://doi.org/10.1016/j.rse.2006.12.006>
- Minsley, B.J., Pastick, N.J., Wylie, B.K., Brown, D.R.N. & Kass, M.A. (2016) Evidence for nonuniform permafrost degradation after fire in boreal landscapes. *Journal of Geophysical Research*, **121**, 320–335. <https://doi.org/10.1002/2015JF003781>
- Murphy, K.A., Reynolds, J.H. & Koltun, J.M. (2008) Evaluating the ability of the differenced Normalized Burn Ratio (dNBR) to predict ecologically significant burn severity in Alaskan boreal forests. *International Journal of Wildland Fire*, **17**, 490–499.
- Nemani, R.R. & Running, S.W. (1997) Land cover characterization using multitemporal red, near-IR, and thermal-IR data from NOAA/AVHRR. *Ecological Applications*, **7**(February), 79–90.
- Parks, S.A., Dillon, G. & Miller, C. (2014) A new metric for quantifying burn severity: the relativized burn ratio. *Remote Sensing*, **6**(3), 1827–1844. <https://doi.org/10.3390/rs6031827>
- Parks, S.A., Holsinger, L.M., Koontz, M.J., Collins, L., Whitman, E., Parisien, M.-A. et al. (2019) Giving ecological meaning to satellite-derived fire severity metrics across North American forests. *Remote Sensing*, **11**(14), 1735. <https://doi.org/10.3390/rs11141735>
- Parks, S.A., Holsinger, L.M., Voss, M.A., Loehman, R.A. & Robinson, N.P. (2018) Mean composite fire severity metrics computed with Google Earth Engine offer improved accuracy and expanded mapping potential. *Remote Sensing*, **10**(879), 1–15. <https://doi.org/10.3390/rs10060879>
- Pérez-Romero, J., Navarro-Cerrillo, R.M., Palacios-rodriguez, G., Acosta, C. & Mesas-Carrascosa, F.J. (2019) Improvement of remote sensing-based assessment of defoliation of *Pinus* spp. caused by *Thaumetopoea pityocampa* Denis and Schiff ermüller and related environmental drivers in Southeastern Spain. *Remote Sensing*, **11**(1736), 1–18.
- Picotte, J.J., Bhattarai, K., Howard, D., Lecker, J., Epting, J., Quayle, B. et al. (2020) Changes to the Monitoring Trends in Burn Severity program mapping production procedures and data products. *Fire Ecology*, **16**, 16. <https://doi.org/10.1186/s42408-020-00076-y>
- Pinno, B.D. & Errington, R.C. (2016) Burn severity dominates understory plant community response to fire in xeric jack pine forests. *Forests*, **7**, 1–14. <https://doi.org/10.3390/f7040083>
- Potapov, P., Hansen, M.C., Laestadius, L., Turubanova, S., Yaroshenko, A., Thies, C. et al. (2017) The last frontiers of wilderness: tracking loss of intact forest landscapes from 2000 to 2013. *Science Advances*, **3**(1), 1–14.
- R Development Core Team. (2021) *R: a language and environment for statistical computing*. Vienna, Austria: R Foundation for Statistical Computing. <https://www.R-project.org/>
- Randerson, J.T., Liu, H., Flanner, M.G., Chambers, S.D., Jin, Y., Hess, P.G. et al. (2006) The impact of boreal forest fire on climate warming. *Science*, **314**(November), 1130–1133.
- Rogers, B.M., Veraverbeke, S., Azzari, G., Czimczik, C.I., Holden, S.R., Mouteva, G.O. et al. (2014) Quantifying fire-wide carbon emissions in interior Alaska using field measurements and Landsat imagery. *Journal of Geophysical Research: Biogeosciences*, **119**, 1608–1629. <https://doi.org/10.1002/2014JG002657>. Received
- Russell, K.L.M. & Johnson, C.J. (2019) Post-fire dynamics of terrestrial lichens: implications for the recovery of woodland caribou winter range. *Forest Ecology and Management*, **434**, 1–17. <https://doi.org/10.1016/j.foreco.2018.12.004>
- Searle, E.B. & Chen, H.Y.H. (2017) Persistent and pervasive compositional shifts of western boreal forest plots in Canada. *Global Ecology and Biogeography*, **23**, 857–866. <https://doi.org/10.1111/gcb.13420>
- Serreze, M.C. & Barry, R.G. (2011) Processes and impacts of Arctic amplification: a research synthesis. *Global and Planetary Change*, **77**, 85–96. <https://doi.org/10.1016/j.gloplacha.2011.03.004>
- Soulard, C.E., Albano, C.M., Villareal, M.L. & Walker, J.J. (2016) Landsat monitoring to assess fire effects on meadows in Yosemite National Park, California. *Remote Sensing*, **8**(5), 371. <https://doi.org/10.3390/rs8050371>
- Soverel, N.O., Perrakis, D.D.B. & Coops, N.C. (2010) Estimating burn severity from Landsat dNBR and RdNBR indices across western Canada. *Remote Sensing of Environment*, **114**, 1896–1909. <https://doi.org/10.1016/j.rse.2010.03.013>
- Spellman, K.V., Mulder, C.P.H. & Hollingsworth, T.N. (2014) Susceptibility of burned black spruce (*Picea mariana*) forests to non-native plant invasions in interior Alaska. *Biological Invasions*, **16**(9), 1879–1895. <https://doi.org/10.1007/s10530-013-0633-6>

- Stocks, B.J., Mason, J.A., Todd, J.B., Bosch, E.M., Wotton, B.M., Amiro, B.D. et al. (2002) Large forest fires in Canada, 1959–1997. *Journal of Geophysical Research: Atmospheres*, **107**, 8149. <https://doi.org/10.1029/2001jd000484>
- Stralberg, D., Wang, X., Parisien, M.-A., Robinne, F.-N., Solyomos, P., Mahon, C.L. et al. (2018) Wildfire-mediated vegetation change in boreal forests of Alberta, Canada. *Ecosphere*, **9**(3), e02156. <https://doi.org/10.1002/ecs2.2156>
- Sulla-Menashe, D., Friedl, M.A. & Woodcock, C.E. (2016) Sources of bias and variability in long-term Landsat time series over Canadian boreal forests. *Remote Sensing of Environment*, **177**, 206–219. <https://doi.org/10.1016/j.rse.2016.02.041>
- Thom, D. & Seidl, R. (2016) Natural disturbance impacts on ecosystem services and biodiversity in temperate and boreal forests. *Biological Reviews of the Cambridge Philosophical Society*, **91**, 760–781. <https://doi.org/10.1111/brv.12193>
- Venier, L.A., Walton, R., Thompson, I.D., Arsenaault, A. & Titus, B.D. (2018) A review of the intact forest landscape concept in the Canadian boreal forest: its history, value, and measurement. *Environmental Reviews*, **26**(July), 369–377.
- Veraverbeke, S., Rogers, B.M., Goulden, M.L., Jandt, R.R., Miller, C.E., Wiggins, E.B. et al. (2017) Lightning as a major driver of recent large fire years in North American boreal forests. *Nature Climate Change*, **7**, 529–534. <https://doi.org/10.1038/nclimate3329>
- Verbyla, D.L., Kasischke, E.S. & Hoy, E.E. (2008) Seasonal and topographic effects on estimating fire severity from Landsat TM/ETM+ data. *International Journal of Wildland Fire*, **17**, 527–534.
- Viereck, L.A. (1983) The effects of fire in black spruce ecosystems of Alaska and northern Canada. In: Wein, D.A. & MacLean, R.W. (Eds.) *The role of fire in northern circumpolar ecosystems*. New York, NY: John Wiley and Sons, pp. 201–220.
- Wang, G.G. & Kembal, K.J. (2005) Effects of fire severity on early development of understory vegetation. *Canadian Journal of Forest Research*, **35**, 254–262. <https://doi.org/10.1139/X04-177>
- Watson, J.E.M., Evans, T., Venter, O., Williams, B., Tulloch, A., Stewart, C. et al. (2018) The exceptional value of intact forest ecosystems. *Nature Ecology & Evolution*, **2**, 599–610.
- Wells, J.V., Dawson, N., Culver, N., Reid, F.A., Siegers, S.M., Kane, E.S. et al. (2020) The state of conservation in North America's boreal forest: issues and opportunities. *Frontiers in Forests and Global Change*, **3**(July), 1–18. <https://doi.org/10.3389/ffgc.2020.00090>
- White, J.D., Ryan, K.C., Key, C.C. & Running, S.W. (1996) Remote sensing of forest fire severity and vegetation recovery. *International Journal of Wildland Fire*, **6**(3), 125–136. <https://doi.org/10.1071/WF9960125>
- Whitman, E., Parisien, M.-A., Holsinger, L.M., Park, J. & Parks, S.A. (2020) A method for creating a burn severity atlas: an example from Alberta, Canada. *International Journal of Wildland Fire*, **29**, 995–1005.
- Whitman, E., Parisien, M., Thompson, D.K. & Flannigan, M.D. (2019) Short-interval wildfire and drought overwhelm boreal forest resilience. *Scientific Reports*, **9**, 18796. <https://doi.org/10.1038/s41598-019-55036-7>
- Whitman, T., Whitman, E., Woolet, J., Flannigan, M.D., Thompson, D.K. & Parisien, M.A. (2019) Soil bacterial and fungal response to wildfires in the Canadian boreal forest across a burn severity gradient. *Soil Biology and Biochemistry*, **138**, 107571. <https://doi.org/10.1016/j.soilbio.2019.107571>
- Xiao, J. & Zhuang, Q. (2007) Drought effects on large fire activity in Canadian and Alaskan forests. *Environmental Research Letters*, **2**, 044003. <https://doi.org/10.1088/1748-9326/2/4/044003>
- Ziel, R.H., Bieniek, P.A., Bhatt, U.S., Strader, H., Rupp, T.S. & York, A. (2020) A comparison of fire weather indices with MODIS fire days for the natural regions of Alaska. *Forests*, **11**(5), 516. <https://doi.org/10.3390/F11050516>

## Supporting Information

Additional supporting information may be found online in the Supporting Information section at the end of the article.

**Table S1.** Number of scenes contributing to pre- and post-fire image for the hybrid and extended composite methods.

**Figure S1.** Non-linear least-squares regression models of the field-based Composite Burn Index as a function of dNBR and RBR severity metrics for the hybrid and extended composite methods, and the paired-scene method for fires from 2002 to 2019 in the boreal region of Alaska.

**Figure S2.** Non-linear least-squares regression models of the field-based Composite Burn Index as a function of dNBR and RBR severity metrics for the hybrid and extended composite methods, and the paired-scene method for fires from 2002 to 2019 in the boreal region of Canada.